

Three-dimensional singularities of a thin plasma slab

F. Pegoraro,¹ S. V. Bulanov,² J. I. Sakai,³ and G. Tomassini⁴

¹*Physics Department of the University of Pisa and INFN, Pisa 56100, Italy*

²*General Physics Institute—RAS, Moscow 119991, Russia*

³*Faculty of Engineering, Toyama University, Toyama 930, Japan*

⁴*Scuola Normale Superiore, Pisa 56100, Italy*

(Received 22 December 2000; revised manuscript received 26 March 2001; published 26 June 2001)

The three-dimensional (3D) nonlinear development of the interchangelike (Rayleigh-Taylor) instability of a thin slab of plasma exhibits interesting features with respect to its two-dimensional (2D) limit investigated by Bulanov, Pegoraro, and Sakai [Phys. Rev. E **59**, 2292 (1999)]. We show that, contrary to the 2D case, the 3D evolution equations remain nonlinear when Lagrangian variables are adopted. Explicit solutions are found by the use of a generalized hodograph transformation. Both compression and rarefaction singularities are formed. Local solutions in the neighborhood of the singular points have a generic 2D character.

DOI: 10.1103/PhysRevE.64.016415

PACS number(s): 95.30.Qd, 47.20.Ky, 52.35.Tc, 52.35.Py

I. INTRODUCTION

The formation of finite time singularities, and the characterization of their spatial structure, represent one of the most interesting problems in the study of the time evolution of nonlinear systems. The Rayleigh-Taylor instability of a thin plasma slab [1,2] provides one of the best examples of the basic nonlinear behavior of a fluid when its equilibrium configuration is unstable against infinitesimal perturbations. In addition, in some simplified limits, it is amenable to exact mathematical solutions that make it possible to study the formation and properties of singularities produced in the nonlinear evolution of the instability. In Ref. [2] Sec. II, the model of a thin slab of weakly ionized plasma moving under the pressure of a magnetic field in a background of neutral gas, providing a strong friction force, was considered. The use of the thin shell approximation, developed in Refs. [1,3,4] and [5], and the simplifying assumption that the shell configuration remains constant along one spatial (Cartesian) direction [two-dimensional (2D) approximation] allowed the authors of Ref. [2] to give an explicit analytical description of the nonlinear aspects of the Rayleigh-Taylor instability in a 2D configuration in the long wavelength approximation. In this 2D configuration the magnetic field was taken to be constant, and to be aligned along the symmetry direction y . It was shown that the *nonlinear* development of the instability is described by a set of two *linear* equations relating the position of an element of the shell in the x - z plane to the time t and to the Lagrangian coordinate α marking the shell element. The solutions of these equations can be expressed in terms of the real and imaginary parts of an analytic function of a complex variable [7]. This function corresponds to a conformal transformation between the (α, t) and (x, z) planes. This analytical function leads to the appearance of singularities. It was shown that two types of singularities are possible: compression singularities, where the surface density of the shell tends to infinity; and rarefaction singularities, corresponding to a tearing of the shell at the position where its surface density goes to zero. The occurrence of finite time singularities, as opposed to singularities that develop as $t \rightarrow \infty$, and the ill posedness of the initial conditions were also discussed. In this analysis the fact that the friction

force is dominant on the inertia terms and the long wavelength approximation plays an important role, by making the mode growth rate increase linearly with the mode wave number.

The extension of these results to a fully 3D configuration, where the shape of the shell representing the thin plasma slab is not assumed to remain constant along one spatial (Cartesian) direction is nontrivial. First the dynamics of the magnetic field pushing the plasma slab is essentially different in a 3D configuration. Second, the kinematics of the foil remains nonlinear, as shown below, even when the conformal transformation method is suitably generalized.

Regarding the first point, in the present paper the extension to the 3D case is obtained by referring to a scalar effective pressure pushing the plasma shell. Furthermore, it is assumed that the pressure at the slab surface is spatially uniform, although it may vary with time. The three-dimensional evolution of a plasma shell, pushed by the electromagnetic radiation pressure against a background of neutral atoms that provides the friction force, is an example of such a physical system, and is of interest for space plasma conditions such as, e.g., in the case of the interaction of the tail of a comet with the solar radiation [6].

Regarding the second point, in the 2D case the pressure force acts essentially on a curve (the projection of the shell in the plane perpendicular to the direction of symmetry) and is thus a linear function of size. In three dimensions the pressure force acts on a surface, and is thus a quadratic function of size. Due to this different scaling with size, in three dimensions the evolution equations for the position in space $\mathbf{r}=(x, y, z)$ of a shell element do not become linear, in contrast to the 2D case, when expressed in terms of time t and of the Lagrangian coordinates α and β marking the shell element. Because of this nonlinearity, in three dimensions it is not possible to give a general class of solutions in explicit form as was done in two dimensions in terms of analytical functions of a complex variable. However, general properties of the solutions can nevertheless be identified analytically, and explicit solutions can be found in terms of a generalized hodograph transformation that interchanges dependent and independent variables, i.e., by solving for t , α , and β as functions of x , y , and z .

The main problem we address in this paper in the study of 3D configurations is the formation of singularities. We recover both compression and rarefaction singularities found in Ref. [2] and, by a proper expansion of the solutions in the neighborhood of the singularities, we show that both compression and rarefaction singularities have a generic 2D character: they tend to develop along a curve, and the plasma dynamics in the plane perpendicular to these curves is the same as for a 2D configuration.

This paper is organized as follows: in Sec. II we recall the equations of motion of a thin plasma shell moving in three-dimensional space under the action of a spatially uniform scalar pressure and a strong friction force. In Sec. III we write the 3D shell equations in a coordinate free formulation using the formalism of the external forms of differential geometry. This formulation proves to be a natural one for the problem under examination, and allows us to focus on the differences between the 2D and 3D equations, and to introduce a generalized hodograph transformation in the simplest possible way. The convenience of using the notation of external forms even in the case of the standard hodograph transformation in 1D gasdynamics is illustrated in Appendix A. Explicit solutions of the 3D shell equations are derived and discussed in Sec. IV (also see Appendix B), and for the hodograph transformed equations in Sec. V. The 2D character of the spatial structure of the compression and of the rarefaction singularities in three dimensions is discussed in Sec. VI. Finally the conclusions are given in Sec. VII, together with a discussion of the limitations introduced in the present analysis, by assuming that the pressure remains spatially uniform.

II. GOVERNING EQUATIONS

In this section we derive evolution equations for the 3D plasma slab configuration, under the effect of a scalar pressure force balanced by a strong friction force on a neutral inert background. Neglecting the effect of plasma inertia in comparison to the friction force, as done in Ref. [2], we write the equations governing the nonlinear evolution of the plasma slab in the thin shell approximation introduced in Refs. [1,3], as

$$\nu^{(in)} \sigma \mathbf{v} = \mathcal{P} \mathbf{n} \quad (1)$$

and

$$\frac{d}{dt}(\sigma \mathbf{d}\Sigma) = 0, \quad (2)$$

where \mathbf{v} is the velocity of the shell, σ its mass density for unit surface, \mathcal{P} is the pressure jump through the plasma slab with respect to the normal vector \mathbf{n} , $\nu^{(in)}$ is the friction frequency, d/dt is the Lagrangian time derivative, and $\mathbf{d}\Sigma$ is the (oriented) surface element on the shell. Equations (1) and (2) have 1D solutions that describe stationary regimes of motion of the types

$$\sigma = \text{const}, \quad z - Vt = \text{const}, \quad (3)$$

where the motion has been taken along z , and $V = \mathcal{P}/(\sigma \nu^{(in)})$. These configurations are unstable against a Rayleigh-Taylor type instability, similar to the interchange instability of a fluid plasma supported against gravity by a magnetic field [8].

As already mentioned in Ref. [2], the thin shell approximation is appropriate in order to analyze the nonlinear development of the Rayleigh-Taylor instability of a plasma slab in the long wavelength approximation, where the perturbation wavelength is much larger than the slab width L . This approach was developed in Ref. [1] in the case of a plasma where inertia, and not friction, balances the externally applied pressure. A discussion of the validity of this approximation during the nonlinear evolution of the instability, in the case of compression and rarefaction singularities in two dimensions, can be found in Ref. [2].

We consider a 3D case where the shell position depends on all three spatial coordinates x, y , and z and on time t . We assume that the shell is initially located on a smooth surface that we parametrize as $z = \mathcal{Z}(x, y)$. We simplify the problem of the shell evolution by assuming that the pressure jump \mathcal{P} along \mathbf{n} remains spatially uniform along the shell, so that $\mathcal{P} = \mathcal{P}(t)$. The more general case where \mathcal{P} depends on the coordinates on the shell surface is briefly discussed in Eq. (23), and in the conclusions.

In order to obtain equations for the shell evolution, we introduce the Lagrange variables α and β , related to the Euler coordinates by

$$x = x(\alpha, \beta, t), \quad y = y(\alpha, \beta, t), \quad \text{and} \quad z = z(\alpha, \beta, t), \quad (4)$$

where α and β are a set of variables marking the shell elements. Convenient choices of α and β are given, e.g., by a set of (local) orthogonal coordinates on the surface where the shell is located at $t=0$. In the simple case where the shell is initially planar we can choose $\mathcal{Z} \equiv 0$ and $x = \alpha$ and $y = \beta$ at $t=0$.

We consider a small plaquette on the shell, centered around the point with Lagrangian coordinates α and β , and with area $d\Sigma_0$. At time t the center of the plaquette is located at x, y , and z , with area $d\Sigma$. In Lagrange variables, from Eq. (2) for the surface mass density σ we obtain

$$\sigma_0 d\Sigma_0 = \sigma d\Sigma, \quad (5)$$

where σ_0 is the initial surface density of the shell expressed in terms of the Lagrangian coordinates α and β , with

$$d\Sigma_0 = |d\alpha \times d\beta| \quad \text{and} \quad d\Sigma = |dx \times dy, dy \times dz, dz \times dx|, \quad (6)$$

the initial area of the plaquette and its area at time t . From Eq. (5) we obtain

$$\begin{aligned}\sigma &= \sigma_0 \frac{d\Sigma_0}{d\Sigma} \\ &= \sigma_0 \left[\left(\frac{\partial x}{\partial \alpha} \frac{\partial y}{\partial \beta} - \frac{\partial y}{\partial \alpha} \frac{\partial x}{\partial \beta} \right)^2 + \left(\frac{\partial y}{\partial \alpha} \frac{\partial z}{\partial \beta} - \frac{\partial z}{\partial \alpha} \frac{\partial y}{\partial \beta} \right)^2 \right. \\ &\quad \left. + \left(\frac{\partial z}{\partial \alpha} \frac{\partial x}{\partial \beta} - \frac{\partial x}{\partial \alpha} \frac{\partial z}{\partial \beta} \right)^2 \right]^{-1/2}.\end{aligned}\quad (7)$$

Then, from Eq. (1), using Eq. (7) with $\mathbf{d}\Sigma = d\Sigma \mathbf{n}$, we obtain the equations of motion

$$\frac{\partial x}{\partial \tau} = \{y, z\}_{\alpha, \beta}, \quad \frac{\partial y}{\partial \tau} = \{z, x\}_{\alpha, \beta}, \quad \frac{\partial z}{\partial \tau} = \{x, y\}_{\alpha, \beta}, \quad (8)$$

where the Poisson brackets with respect to the Lagrange variables α and β are defined by

$$\{ \cdot, \cdot \}_{\alpha, \beta} \equiv \frac{\partial}{\partial \alpha} \frac{\partial}{\partial \beta} - \frac{\partial}{\partial \beta} \frac{\partial}{\partial \alpha}, \quad (9)$$

and the normalized time variable has been defined as

$$\tau = \int^t \frac{\mathcal{P}(t)}{\sigma_0 v^{(in)}} dt. \quad (10)$$

In deriving Eq. (8) we have assumed that the Lagrangian variables α and β have been chosen in such a way that σ_0 is spatially constant (say $\sigma_0 \equiv 1$). This is analogous to the choice of the mass variable m introduced in Ref. [2]. This freedom in the definition of α and β allows us to include in this treatment shells with a nonuniform initial density distribution. Similarly structured equations, though involving second derivatives with respect to τ instead of first derivatives, were obtained in the case of a shell pushed by a scalar pressure in Ref. [3], and analyzed in Ref. [4] in the case of the Rayleigh-Taylor instability of a fully ionized thin plasma shell where the pressure is balanced by the plasma inertia.

If x and z are independent of β , we obtain $y \equiv \beta$ (i.e., $\partial y / \partial \beta \equiv 1$), and we recover the linear 2D equations derived in Ref. [2],

$$\frac{\partial x}{\partial \tau} = -\frac{\partial z}{\partial \alpha} \quad \text{and} \quad \frac{\partial z}{\partial \tau} = \frac{\partial x}{\partial \alpha}, \quad (11)$$

which are simply the Cauchy-Riemann conditions for the real and imaginary parts of an analytical function $W(\zeta)$ of a complex variable:

$$\zeta = \alpha + i\tau. \quad (12)$$

The real part of $W(\zeta)$ is equal to the x coordinate of the foil, while the z coordinate is the imaginary part. Thus we can write

$$x + iz = W(\zeta). \quad (13)$$

The complex function W gives a conformal mapping from the complex plane $\alpha + i\tau$ to the plane $x + iz$, and x and z are harmonic functions of α and τ , i.e.,

$$\frac{\partial^2 x}{\partial \alpha^2} + \frac{\partial^2 x}{\partial \tau^2} = \frac{\partial^2 z}{\partial \alpha^2} + \frac{\partial^2 z}{\partial \tau^2} = 0. \quad (14)$$

If, instead, β is not an ignorable coordinate, and x and z depend on β , the equations of motion of the thin shell remain nonlinear, with a ‘‘vector type’’ nonlinearity given by the expressions inside the Poisson brackets.

Equations (8) satisfy the constraint

$$\left\{ \frac{\partial x}{\partial \tau}, x \right\}_{\alpha, \beta} + \left\{ \frac{\partial y}{\partial \tau}, y \right\}_{\alpha, \beta} + \left\{ \frac{\partial z}{\partial \tau}, z \right\}_{\alpha, \beta} = 0, \quad (15)$$

which follows from the Jacobi identity obeyed by the Poisson Brackets. In the 2D limit each term of this expression is identically zero. In Eulerian coordinates, in terms of the velocity $\mathbf{v} \equiv \partial \mathbf{r} / \partial \tau$, constraint (15) takes the form

$$\mathbf{v} \cdot \nabla \times \mathbf{v} = 0, \quad (16)$$

i.e., the helicity of the shell velocity field is zero, and \mathbf{v} admits orthogonal surfaces, as implicit in our shell problem.

III. 3D EQUATIONS IN COORDINATE-FREE FORM

In order to study the properties of Eqs. (8), and to devise methods for solving them, it is convenient to rewrite Eqs. (8) in the coordinate free notation of differential geometry [9]. This formulation will allow us to compare the 2D and 3D cases more simply, and to obtain an extension of the hodograph transformation [10]. The use of the hodograph transformation, where dependent and independent variables are interchanged, is well known in the simpler case of two independent variables and two dependent variables, e.g., in 1D gasdynamics, in which case it leads to linear equations for the fluid space coordinate and for time as functions of the fluid velocity and density, as briefly recalled in Appendix A.

The hodograph transformation was used in Ref. [2] to show that the 2D equations (11) can be rewritten in terms of the inverse conformal mapping W^{-1} from the complex $x + iz$ plane to the $\alpha + i\tau$ plane and that, with this change of dependent and independent variables, α and τ are harmonic functions of x and z , i.e.,

$$\frac{\partial^2 \alpha}{\partial x^2} + \frac{\partial^2 \alpha}{\partial z^2} = \frac{\partial^2 \tau}{\partial x^2} + \frac{\partial^2 \tau}{\partial z^2} = 0. \quad (17)$$

In three dimensions the hodograph transformed equations can be obtained by expressing α , β , and τ as functions of x, y , and z . This transformation will allow us to show that the main property of the evolution equations, that is preserved in the generalization from two to three dimensions, is

$$\nabla^2 \tau = 0, \quad (18)$$

where the Laplace operator is taken with respect to x and z in two dimensions and x, y , and z in three dimensions.

To prove these results, first we show that Eqs. (8) can be written in the notation of differential forms as the equality of

three 3 forms involving exterior products of the 1 forms obtained by differentiating the independent and the dependent variables,

$$\begin{aligned} dx \wedge d\alpha \wedge d\beta &= d\tau \wedge dy \wedge dz, \\ dy \wedge d\alpha \wedge d\beta &= d\tau \wedge dz \wedge dx, \\ dz \wedge d\alpha \wedge d\beta &= d\tau \wedge dx \wedge dy, \end{aligned} \quad (19)$$

where now d denotes the exterior derivative, and \wedge the exterior product (for a detailed definition of these operations, see, e.g., Ref. [9]).

In order to recover Eqs. (8) we express the 1 form dx in terms of the three 1 forms $d\alpha$, $d\beta$, and $d\tau$, as

$$dx = \frac{\partial x}{\partial \alpha} d\alpha + \frac{\partial x}{\partial \beta} d\beta + \frac{\partial x}{\partial \tau} d\tau, \quad (20)$$

and, analogously for dy and dz , we insert these expressions into Eqs. (19) and use the antisymmetric properties of the exterior product.

Note that Eq. (7) becomes simpler in the differential form notation, and can be rewritten as

$$\begin{aligned} \sigma_0 |d\alpha \wedge d\beta| &= \sigma |dx \wedge dy + dy \wedge dz + dz \wedge dx| \\ &= \sigma |d\alpha \wedge d\beta| \sqrt{(\{x,y\}_{\alpha,\beta}^2 + \{y,z\}_{\alpha,\beta}^2 + \{z,x\}_{\alpha,\beta}^2)}, \end{aligned} \quad (21)$$

i.e.,

$$\sigma = \sigma_0 \left(\left| \frac{\partial x}{\partial \tau} \right|^2 + \left| \frac{\partial y}{\partial \tau} \right|^2 + \left| \frac{\partial z}{\partial \tau} \right|^2 \right)^{-1/2}, \quad (22)$$

which can be simply interpreted in terms of the continuity equation.

We note that, in the case of a pressure jump that evolves in time, becoming spatially nonuniform, Eqs. (19) take the more general form

$$\sigma_0 \sqrt{(\{\alpha,\beta\}_{x,y}^2 + \{\alpha,\beta\}_{y,z}^2 + \{\alpha,\beta\}_{z,x}^2)} |dx \wedge dy + dy \wedge dz + dz \wedge dx| = \sigma |dx \wedge dy + dy \wedge dz + dz \wedge dx|, \quad (29)$$

which gives

$$\sigma = \sigma_0 |\nabla \tau|. \quad (30)$$

Hodograph transformation in two and three dimensions

In the two-dimensional case, $d\beta \equiv dy$, and the system of equations (19) reduces to the equality between two 2 forms,

$$dx \wedge d\alpha = dz \wedge d\tau, \quad dz \wedge d\alpha = d\tau \wedge dx, \quad (31)$$

while Eqs. (11) are reobtained by inserting

$$dx \wedge d\alpha \wedge d\beta = \mathcal{F}(\alpha, \beta, t) dt \wedge dy \wedge dz, \quad (23)$$

and similarly for the remaining two equations. Here $\mathcal{F}(\alpha, \beta, t) \equiv \mathcal{P}(\alpha, \beta, t)/\sigma_0$, and the time evolution of $\mathcal{P}(\alpha, \beta, t)$ must be determined from the dynamics of the term exerting the pressure force on the shell.

If we interchange dependent and independent variables, and write

$$d\alpha = \frac{\partial \alpha}{\partial x} dx + \frac{\partial \alpha}{\partial y} dy + \frac{\partial \alpha}{\partial z} dz, \quad (24)$$

and, analogously for $d\beta$ and $d\tau$, insert these expressions into Eqs. (19) and again use the antisymmetric properties of the exterior product, we obtain the hodograph transformed equations

$$\begin{aligned} \frac{\partial \tau}{\partial x} &= \frac{\partial \alpha}{\partial y} \frac{\partial \beta}{\partial z} - \frac{\partial \beta}{\partial y} \frac{\partial \alpha}{\partial z}, \\ \frac{\partial \tau}{\partial y} &= \frac{\partial \alpha}{\partial z} \frac{\partial \beta}{\partial x} - \frac{\partial \beta}{\partial z} \frac{\partial \alpha}{\partial x}, \quad \frac{\partial \tau}{\partial z} = \frac{\partial \alpha}{\partial x} \frac{\partial \beta}{\partial y} - \frac{\partial \beta}{\partial x} \frac{\partial \alpha}{\partial y}. \end{aligned} \quad (25)$$

These can be combined in the vector equation

$$\nabla \tau = \nabla \alpha \times \nabla \beta, \quad (26)$$

where $\nabla \tau$ denotes the gradient of the function $\tau = \tau(x, y, z)$ in x, y, z space, etc. From Eq. (26) we obtain Eq. (18) by applying the divergence operator ∇ , and by noting that the right hand side of Eq. (26) can be written as $\nabla \times (\alpha \nabla \beta)$. From Eq. (26), we also obtain

$$\nabla \tau \cdot \nabla \alpha = \nabla \tau \cdot \nabla \beta = 0 \quad (27)$$

and the τ -independent compatibility equation

$$\nabla \times (\nabla \alpha \times \nabla \beta) = 0. \quad (28)$$

Note that, in contrast to the 2D case, where all variables play the same role, in general $\nabla^2 \alpha \neq 0$ and $\nabla^2 \beta \neq 0$. In terms of the hodograph transformed equations Eq. (7) takes the form

$$dx = \frac{\partial x}{\partial \alpha} d\alpha + \frac{\partial x}{\partial \tau} d\tau, \quad (32)$$

and the analogous expression for dz , into Eqs. (31). The hodograph transformed equations are obtained by inserting

$$d\alpha = \frac{\partial \alpha}{\partial x} dx + \frac{\partial \alpha}{\partial z} dz, \quad (33)$$

and the analogous expression for $d\tau$, into Eqs. (31), and read

$$\frac{\partial \tau}{\partial x} = -\frac{\partial \alpha}{\partial z}, \quad \frac{\partial \tau}{\partial z} = \frac{\partial \alpha}{\partial x}. \quad (34)$$

Note that in two dimensions Eqs. (11) and their hodograph transformed form [Eq. (34)] have the same mathematical structure. In particular they correspond to Cauchy-Riemann conditions for the real and imaginary parts of an analytical function W and of its inverse W^{-1} , respectively. Conversely, in three dimensions Eqs. (8) and (26) are mathematically different: Eqs. (8) are algebraic in nature, and are expressed in terms of Poisson brackets, while Eqs. (26) are best interpreted geometrically in terms of two pairs of orthogonal surfaces [$\alpha = \alpha(x, y, z)$, $\tau = \tau(x, y, z)$] and [$\beta = \beta(x, y, z)$, $\tau = \tau(x, y, z)$], such that the vector product of the gradients of α and β is equal to the gradient of τ .

IV. SOLUTIONS OF THE 3D THIN SHELL EQUATIONS

A. Stationary solutions and linearized equations

The steady, rigid motion of the thin shell is recovered from Eqs. (8) by taking $x = \alpha$, $y = \beta$, and $z = \tau$. This solution is unstable against infinitesimal perturbations, as can be shown by linearizing Eqs. (8). This leads to the following system of equations for the displacement vector ξ :

$$\frac{\partial \xi_x}{\partial \tau} = -\frac{\partial \xi_z}{\partial \alpha}, \quad \frac{\partial \xi_y}{\partial \tau} = -\frac{\partial \xi_z}{\partial \beta}, \quad \frac{\partial \xi_z}{\partial \tau} = \frac{\partial \xi_x}{\partial \alpha} + \frac{\partial \xi_y}{\partial \beta}, \quad (35)$$

which give

$$\nabla^2 \xi_z = 0 \quad \text{and} \quad \nabla^2 (\partial \xi_x / \partial \tau) = \nabla^2 (\partial \xi_y / \partial \tau) = 0, \quad (36)$$

where the Laplace operator is taken with respect to the variables α , β , and τ . Equations (36) correspond to a linear dispersion equation of the form $\gamma^2 = k_x^2 + k_y^2$, where γ is the (normalized) mode growth rate and $k_{x,y}$ are the mode (normalized) wave numbers in the shell plane. Note that the structural difference between the 2D and 3D equations is not seen at this linear level.

In the fully nonlinear case explicit solutions of Eqs. (8) are not easy to find. On the contrary, explicit nonlinear solutions of the hodograph transformed equations will be given in Sec. V.

Below we will consider the special case of Eqs. (8) corresponding to rotational invariance around the z axis which leads to rotationally invariant solutions. In Appendix B it is shown that Eqs. (8) admit self-similar solutions where the shell velocity components are linear, time dependent functions of x, y, z (see, e.g., Refs. [11,12] and references quoted therein).

B. Rotationally invariant solutions

If we assume that the shell evolution is rotationally invariant around the z axis, we can set

$$x = \alpha F(u, \tau), \quad y = \beta F(u, \tau), \quad \text{and} \quad z = G(u, \tau), \quad (37)$$

where $2u \equiv \alpha^2 + \beta^2$. Inserting Eqs. (37) into Eqs. (8), we obtain

$$\frac{\partial G}{\partial u} = -\frac{\partial \ln(F)}{\partial \tau} \quad \text{and} \quad \frac{\partial G}{\partial \tau} = \frac{\partial(u F^2)}{\partial u}, \quad (38)$$

which give the nonlinear elliptic equation

$$\frac{\partial^2 \ln(F)}{\partial \tau^2} + \frac{\partial^2(u F^2)}{\partial u^2} = 0. \quad (39)$$

Equations (38) admit factorized solutions of the forms

$$F(u, \tau) = \frac{(C - u/2)^{1/2}}{\tau_0 - \tau} \quad \text{and} \quad G(u, \tau) = \frac{C - u}{\tau_0 - \tau}, \quad (40)$$

where τ_0 and C are integration constants. This solution describes the ‘‘finite time’’ explosion of a thin spherical shell with radius given by

$$x^2 + y^2 + z^2 \equiv R^2 = \frac{C^2}{(\tau_0 - \tau)^2}. \quad (41)$$

The variables α and β are related to the coordinates on the spherical shell at $\tau = 0$ as

$$\alpha = [2\tau_0(R - z)]^{1/2} \cos \phi, \quad \beta = [2\tau_0(R - z)]^{1/2} \sin \phi, \quad (42)$$

where ϕ is the polar angle in the x - y plane and $\sigma_0 = C$. The inverse dependence of the radius R of the sphere with ‘‘time’’ τ can be easily understood in terms of the equation $\dot{R} \propto R^2$, which expresses the fact that the total ‘‘force’’ is proportional to the sphere surface. Note that if we express τ as the function of t , using Eq. (10), and adopt an equation of the type $\mathcal{P}V^\gamma$, where V is the volume inside the hemispherical volume constant and γ is a polytropic index, we find $R \propto t^{1/(3\gamma-1)}$. Thus, in real time, the shell explosion occurs only for $t \rightarrow \infty$ with a slow algebraic growth.

A different solution which does not exhibit a finite time singularity (in the τ time variable) is given by

$$F(\tau) = F_o \exp(\tau/\tau_0),$$

$$G(u, \tau) = -u/\tau_0 + (F_o^2 \tau_0/2) \exp(2\tau/\tau_0)/2, \quad (43)$$

where F_o and τ_0 are integration constants. This solution describes the evolution of the paraboloidal shell,

$$z - z_o(\tau) = -(x^2 + y^2)/(4z_o(\tau)), \quad (44)$$

with $z_o(\tau) = (F_o^2 \tau_0/2) \exp(2\tau/\tau_0)$. The variables α and β are related to the coordinates on the paraboloidal shell at $\tau = 0$ as in Eq. (42), with $z_o(\tau = 0)$ substituted for $R(\tau = 0)$. The exponential dependence of the vertex of the paraboloid on ‘‘time’’ τ can be understood in terms of the equation $\dot{z} \propto (x^2 + y^2) \propto z$, which expresses the fact that the force is proportional to the area of the surface around the vertex which, in a paraboloid, scales linearly with the vertex position z . For $\tau_0 < 0$, Eq. (43) describes the case where the pressure focal-

izes all the matter in the foil on the negative z -axis at $\tau=\infty$. At $\tau\rightarrow-\infty$ the shell is flat and has a uniform, vanishingly small, density.

V. SOLUTIONS OF THE 3D HODOGRAPH EQUATIONS

The geometrical interpretation of the hodograph transformed equations for the 3D thin shell, $\nabla\tau=\nabla\alpha\times\nabla\beta$, in terms of orthogonal surfaces ($\nabla\alpha\cdot\nabla\tau=\nabla\beta\cdot\nabla\tau=0$) makes it easier to find families of explicit solutions.

In addition, once a solution is found, we can generate new solutions by exploiting the invariance of the hodograph transformed equations (26) under the transformations of the independent variables

$$\alpha\rightarrow\alpha+H(\beta), \quad \beta\rightarrow\beta, \quad (45)$$

$$\alpha\rightarrow L(\alpha), \quad \beta\rightarrow\frac{\beta}{(dL(\alpha)/d\alpha)}, \quad (46)$$

where H and L are arbitrary functions. An analogous invariance holds when the above transformations are applied to β .

Exponential-type solutions are obtained by taking

$$\begin{aligned} \alpha &= \sqrt{2} \sin(x) \exp(z/\sqrt{2}), \\ \beta &= \sqrt{2} \sin(y) \exp(z/\sqrt{2}), \\ \tau &= \sqrt{2} \cos(x) \cos(y) \exp(z\sqrt{2}), \end{aligned} \quad (47)$$

which can be easily inverted, and give

$$\begin{aligned} z &= \frac{1}{\sqrt{2}} \ln \left(\frac{\alpha^2 + \beta^2 \pm \sqrt{(\alpha^2 - \beta^2)^2 + 8\tau^2}}{4} \right), \\ (x, y) &= \arcsin \left[\frac{(\alpha, \beta)}{[(\alpha^2 + \beta^2)/2 \pm \sqrt{(\alpha^2 - \beta^2)^2/4 + 2\tau^2}]^{1/2}} \right], \end{aligned} \quad (48)$$

where we will consider only the plus sign in front of the square root which is defined to be positive. Physically, for $\tau < 0$, this solution can be taken to represent the evolution of a small square shell that is pushed along z , and that breaks at $\alpha = \beta = 0$ at $\tau = 0$, having reached $z = -\infty$ as shown in Fig. 1. For notational convenience here and below the time variable τ is chosen such that $\tau = 0$ corresponds to the time where the singularity occurs while the initial conditions are given at $\tau = \tau_0 \neq 0$. The logarithmic dependence of the vertex of the shell on time τ around $\alpha = \beta = 0$ can be understood in terms of the equation $\dot{z} \propto (x^2 + y^2) \propto 1/\tau \exp(-z\sqrt{2})$, which expresses the fact that the force is proportional to the area of the surface around the vertex which, in this solution, increases exponentially with the vertex position z for $z < 0$.

Polynomial solutions are obtained by taking

$$\alpha = P_\alpha^n(x, y, z), \quad \beta = P_\beta^m(x, y, z), \quad \tau = P_\tau^p(x, y, z), \quad (49)$$

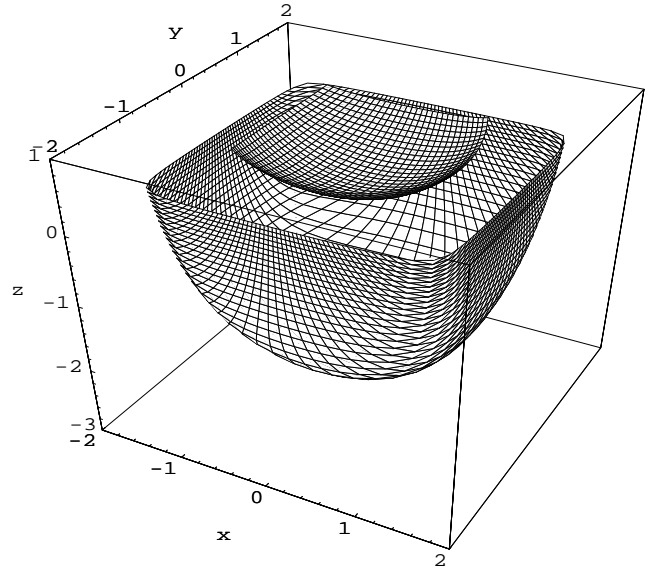


FIG. 1. Time evolution of a small square shell blown along the negative z according to Eq. (48). The position of the shell is shown at two different times.

where p , m , and n , with $p = m + n - 1$, are the orders of the polynomials, and the coefficients of the polynomials P are restricted by the constraints imposed by Eqs. (26). A simple class of such solutions corresponds to $m = n = 2$ and $p = 3$. Using standard index notation and summation over repeated indices, we write

$$2\alpha = A_{ij}x_i x_j, \quad 2\beta = B_{ij}x_i x_j \quad \text{and} \quad 6\tau = T_{ijk}x_i x_j x_k, \quad (50)$$

where the indices vary from 1 to 3, with $x_1 = x$, $x_2 = y$ and $x_3 = z$. From Eqs. (26), we obtain the condition

$$B_{kk}A_{ij} - A_{kk}B_{ij} + A_{ik}B_{kj} - B_{ik}A_{kj} = 0, \quad (51)$$

i.e., the commutation condition $[\hat{A}, \hat{B}] = (\text{tr } \hat{A})\hat{B} - (\text{tr } \hat{B})\hat{A}$, where $\text{tr } \hat{A}$ denotes the trace of the matrix \hat{A} , and

$$T_{ijk} = \epsilon_{ilm}A_{lj}B_{mk}, \quad (52)$$

where the right hand side must be symmetrized with respect to the the indices i , j , and k , and ϵ_{ilm} is the completely antisymmetric Ricci tensor. An interesting solution is given by

$$\alpha = (x^2 - z^2)/2, \quad \beta = (y^2 - z^2)/2, \quad \tau = xyz, \quad (53)$$

which describes a shell that for negative τ has the shape of a symmetric (equilateral) hyperbolic surface in one octant. The density in the shell is proportional to $(x^2 y^2 + y^2 z^2 + z^2 x^2)^{1/2}$. At $\tau = 0$ the position of the shell coincides with its asymptotic quarter-planes and then, after breaking at the origin, opens into three hyperbolic ‘‘petals’’ in the adjacent octants, as shown in Fig. 2. This solution generalizes (in a special symmetric, nongeneric way as will be discussed in Sec. VI B) the 2D finite time rarefaction singularity given by Eq. (56) of Ref. [2].

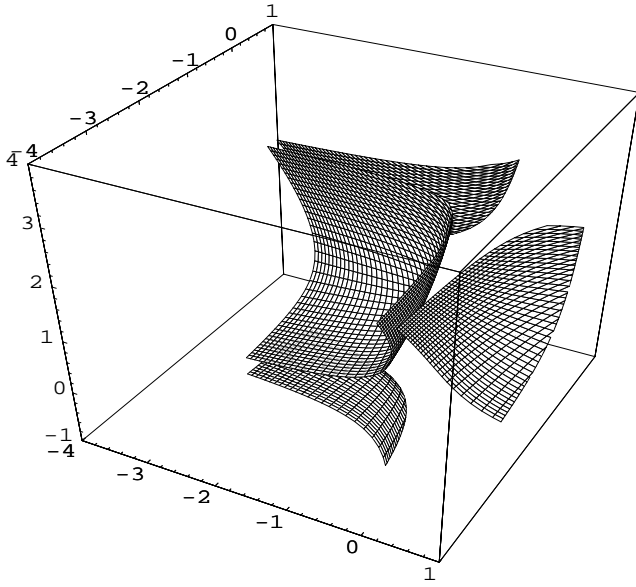


FIG. 2. Time evolution of an equilateral hyperbolic shell moving in the upper left forward octant toward the origin according to Eq. (53), and subsequently splitting into three disconnected “petals” in the adjacent octants. The position of the shell is shown at two different times, before and after breaking.

The well known systems of orthogonal coordinates, that are commonly used in mathematical physics, can be rewritten in such a way as to lead to solutions of Eqs. (26). A spherical solution is obtained by setting

$$\tau = 1/r = 1/(x^2 + y^2 + z^2)^{1/2}, \quad \alpha = \cos \theta = \frac{z}{(x^2 + y^2 + z^2)^{1/2}},$$

$$\beta = \varphi = \arctan(y/x), \quad (54)$$

where r, θ , and φ are the usual spherical coordinates. This solution can be easily verified, since

$$\nabla \tau = -(1/r^2)\mathbf{e}_r, \quad \nabla \alpha = -(\sin \theta/r)\mathbf{e}_\theta,$$

$$\nabla \beta = 1/(r \sin \theta)\mathbf{e}_\phi, \quad (55)$$

with \mathbf{e} the unit vectors along the spherical coordinates. Equation (54) can be inverted, and gives

$$x = \frac{\sin(\arccos \alpha) \cos \beta}{\tau}, \quad y = \frac{\sin(\arccos \alpha) \sin \beta}{\tau}, \quad z = \frac{\alpha}{\tau}. \quad (56)$$

It describes an expanding $r \rightarrow \infty$ for $\tau = 0$ (and a collapsing $r = 0$ for $\tau = \infty$) sphere, and essentially coincides with solution (41) found in Sec. IV B. Azimuthally modulated solutions with the same time behavior can be constructed by applying to β in Eqs. (54) the transformation given by Eq. (46).

The spherical solution [Eq. (54)] can now be used as a starting point for constructing an infinite linear space of azimuthally symmetric solutions that exploit the well known properties of the solutions of the Laplace operator. First we

note that the function τ in Eqs. (54) satisfies, in agreement with Eq. (18), the Laplace equation $\nabla^2 \tau = 0$. Then we recall that if \mathbf{S} is a constant vector, then $(\mathbf{S} \cdot \nabla)\tau$ is also a solution of the Laplace operator. Moreover, if \mathbf{S} is along z , $(\mathbf{S} \cdot \nabla)\beta = 0$, with β given by Eq. (54), and new “multipolar” solutions of Eqs. (26) can be constructed by applying the transformations

$$\tau \rightarrow \frac{\partial^m \tau}{\partial z^m}, \quad \alpha \rightarrow \frac{\partial^m \alpha}{\partial z^m}, \quad \beta \rightarrow \beta. \quad (57)$$

These solutions can be linearly combined in α, β, τ space. When transformed back to x, y, z space, they correspond to nonlinear combinations.

Prolate and oblate ellipsoids can be obtained by applying the operator

$$1 + e \frac{\partial^2}{\partial z^2} \quad (58)$$

to Eq. (54), with e either positive (prolate) or negative (oblate ellipsoids). We obtain

$$\tau = \frac{(x^2 + y^2 + z^2)^2 - e(x^2 + y^2 - 2z^2)}{(x^2 + y^2 + z^2)^{5/2}}, \quad (59)$$

$$\alpha = z \frac{(x^2 + y^2 + z^2)^2 - 3e(x^2 + y^2)}{(x^2 + y^2 + z^2)^{5/2}}, \quad \beta = \arctan(y/x).$$

For small values of τ the ellipsoids become quasispherical. For small negative values of e we obtain an oblate ellipsoid that expands ($\tau \rightarrow 0$)/collapses ($\tau \rightarrow \infty$) along z faster than in the equatorial plane. The collapsing solution develops two symmetric, hyperbolic, finite time singularities along the z axis. As shown in Fig. 3(a), these singularities arise when the collapsing oblate ellipsoid touches an expanding, two-lobed “internal” surface which, for small τ , is approximately given by $(x^2 + y^2 + z^2)^2 = e(x^2 + y^2 - 2z^2)$. For small positive values of e we obtain an expanding ($\tau \rightarrow 0$)/collapsing ($\tau \rightarrow \infty$) prolate ellipsoid. As shown in Fig. 3(b), the collapsing solution breaks at a finite time in the equatorial plane developing a ring-shaped hyperbolic singularity when it touches the expanding, doughnut-shaped “internal” surface.

The procedure of differentiating Eqs. (54) along z can also be reversed. The first integration with respect to z gives a new solution corresponding to the well known parabolic coordinates [13]

$$\tau = \ln(r + z), \quad \alpha = r - z, \quad \beta = \arctan(y/x), \quad (60)$$

which can be inverted for $\alpha \geq 0$, and gives

$$x = \sqrt{\alpha} \exp(\tau/2) \cos \beta, \quad y = \sqrt{\alpha} \exp(\tau/2) \sin \beta, \quad (61)$$

$$z = [\exp(\tau) - \alpha]/2.$$

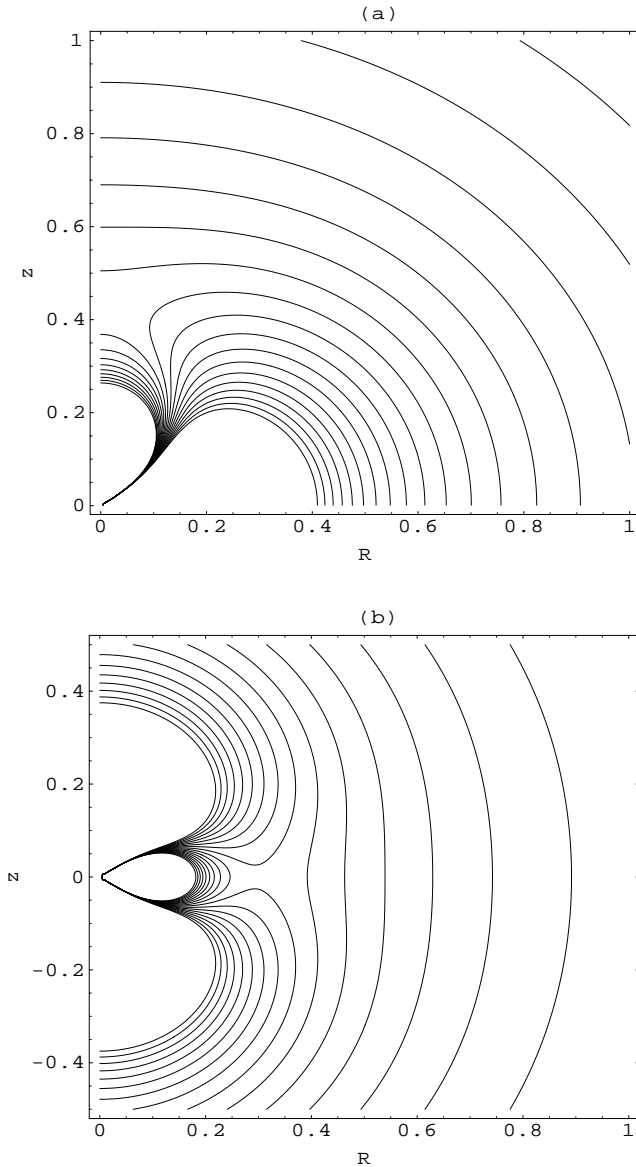


FIG. 3. Time evolution of the poloidal cross section of an oblate (a) and of a prolate (b) ellipsoid expanding ($\tau \rightarrow 0$)/collapsing ($\tau \rightarrow \infty$) according to Eq. (59), with $e = \mp 0.03$. The level curves correspond to the position of the poloidal cross section of the ellipsoids before and after their breaking, which occurs when the ellipsoids touch the “inner surface” expanding along the z axis (a), or equatorially (b).

At the initial time $\tau=0$ this solution corresponds to a paraboloid along the negative z axis, and with vertices at $x=0$, $y=0$, and $z=1/2$ which expand exponentially in time toward large z and large r . This solution is essentially equivalent to the one given by Eq. (43).

Finally we remark that the above solutions are not generic insofar as they are based on some symmetry property. More general solutions are difficult to find: for example, the evolution of a triaxial ellipsoid requires extensive algebraic manipulations based on the so called “ellipsoidal coordinates” used, e.g., in the study of elliptical galaxies (see, e.g., Ref. [14] Part II).

VI. SPATIAL STRUCTURE OF FINITE TIME SINGULARITIES

The special solutions of Eqs. (8) and/or of Eqs. (26) that have been obtained in the previous sections display singularities either at finite time or for $|\tau| \rightarrow \infty$. Two types of singularities appear in these solutions: compression singularities and rarefaction singularities. The first ones occur when the shell density becomes infinite and, according to Eq. (22), correspond to stagnation points where the velocity goes to zero. These singularities are best described in the frame work of Eqs. (8). The second type of singularities correspond to rarefaction singularities where the density vanishes and, according to Eq. (22), $\nabla \tau = 0$, i.e., the velocity diverges. These singularities are best described in the frame work of Eqs. (26). As discussed in Ref. [2] the long wavelength approximation remains valid in the second case, where its accuracy actually improves close to the singularity, while in the first case it loses its validity in the final stage of the development of the singularity and must therefore be interpreted as describing an intermediate asymptotic regime.

A. Finite time compression singularities

Compression singularities occur at the stagnation points where the shell velocity goes to zero. Then Eqs. (8) imply that, at the singularity, the Poisson brackets between x, y , and z vanish, i.e., that locally x, y , and z are not independent functions of α and β . We assume that the compression singularity occurs at $x=0$, $y=0$, and $z=0$, corresponding, with a proper redefinition of the origin of the coordinates, to $\tau=0$, $\alpha=0$, and $\beta=0$. Then, with a proper choice of the independent variables α and β , the functions x, y , and z can be expanded near the compression singularity in the form

$$x_i \approx L_i \alpha + Q_i(\alpha, \beta, \tau), \quad (62)$$

where $x_i = x, y, z$ with $i = (1, 2, 3)$, L_i are numerical coefficients (not all identically zero in the generic case) and Q_i are three quadratic forms of α, β , and τ . The fact that the linear terms are all proportional to the same Lagrangian variable (chosen to be α) and do not depend on τ express the fact that, near $x=0$, $y=0$, and $z=0$, x, y , and z are not independent functions and that the shell velocity vanishes. As in the 2D case discussed in Ref. [2], cubic terms, not explicitly included in Eq. (62) will turn out to be important in the description of a compressional singularity and will be added later.

With a rotation in x, y, z space and a rescaling, we can make $L_j = 0$ for $j \neq 1$ and $L_1 = 1$, i.e., $x = \alpha$ to leading order. Then, inserting Eq. (62) into Eqs. (8), we obtain the following relationships between the coefficients of the quadratic forms Q_i :

$$Q_1^{\tau, \tau} = Q_1^{\alpha, \tau} = Q_1^{\beta, \tau} = 0, \quad (63)$$

and, taking $\lambda = (\alpha, \beta)$,

$$\begin{aligned} Q_2^{\tau,\tau} &= -Q_3^{\beta,\tau}, & Q_2^{\lambda,\tau} &= -Q_3^{\lambda,\beta}, \\ Q_3^{\tau,\tau} &= Q_2^{\beta,\tau}, & Q_3^{\lambda,\tau} &= Q_2^{\lambda,\beta}, \end{aligned} \quad (64)$$

where the upper indices on Q_i refer to the corresponding (symmetric) coefficients of the quadratic form. Equation (63) shows that, to first order, the shell dynamics close to the singularity has a 2D behavior and that, with the coordinate choice made above, occurs in the y - z plane. In this local expansion, the coefficients $Q_1^{\alpha,\alpha}$, $Q_1^{\alpha,\beta}$, $Q_1^{\beta,\beta}$, $Q_2^{\alpha,\alpha}$, and $Q_3^{\alpha,\alpha}$ remain undetermined. With a further rotation around x in the y - z plane we can make $Q_2^{\beta,\tau}=0$. Then Eqs. (64) lead to

$$\begin{aligned} Q_3^{\beta,\beta} &= Q_3^{\tau,\tau}=0, & Q_3^{\beta,\tau} &= Q_2^{\beta,\beta} = -Q_2^{\tau,\tau}, \\ Q_2^{\alpha,\tau} &= -Q_3^{\alpha,\beta}, & Q_3^{\alpha,\tau} &= Q_2^{\alpha,\beta}. \end{aligned} \quad (65)$$

These relationships show that, at $\alpha=0$, y and z are (quadratic) conjugate harmonic functions of β and τ . This result can also be understood by reversing the reasoning leading to Eq. (11). For $\alpha \neq 0$, the dependence of y and z on β and τ remains harmonic, but acquires an α -dependent linear term. This harmonic behavior can be expressed in the form

$$\begin{aligned} y + iz &\approx A\zeta^2 + i2B\alpha\zeta, \quad \text{i.e.,} \\ y + iz &\approx A(\zeta + iB\alpha/A)^2 \equiv A(\zeta')^2 \end{aligned} \quad (66)$$

where $\zeta = \beta + i\tau$ and $\zeta' = \beta' + i\tau' = \zeta + iB\alpha/A$, with $\beta' = \beta$ and $\tau' = \tau$ for $\alpha=0$ and $A \equiv Q_2^{\beta,\beta}$; B is a complex number given by $2B = Q_2^{\alpha,\beta} - iQ_2^{\alpha,\tau}$; and terms proportional to α^2 are supposed to be included in the as yet undetermined coefficients $Q_2^{\alpha,\alpha}$ and $Q_3^{\alpha,\alpha}$.

Equation (66) agrees with the 2D result obtained in Ref. [2]. We recall that in the 2D case the behavior around a finite time compression singularity was analyzed by expanding the function $W(\zeta)$ [see Eq. (13) of the present paper] as

$$W(\zeta) = C_2\zeta^2 + C_3\zeta^3 + \dots, \quad (67)$$

where C_2 and C_3 are complex numbers. It was shown that, in agreement with the standard treatment in the theory of singularities [15], the essential property of the local representation of the mapping from the Lagrange variables to the Euler variables given by Eq. (67) is the cubic dependence on the space Lagrangian coordinate. This dependence determines the 2D cusplike structure of the shell at the singularity [see Eq. (48) of Ref. [2]].

In the present 3-D treatment, the cubic terms in the expression of y and z cannot be expressed in general as harmonic functions of β and τ . Nevertheless, at a critical time $\tau'=0$, retaining linear terms in α , we can include the cubic terms in the forms

$$y = A'(\beta')^2 + C'(\beta')^3 \quad \text{and} \quad z = D\alpha(\beta')^2 + E'(\beta')^3, \quad (68)$$

where A' , C' , and E' are real inhomogeneous linear functions of α that, for $\alpha=0$, are equal to A , C , and E , respec-

tively, A is given in Eq. (66) and C, D , and E are real numbers. In the generic case $E' \neq 0$ while C' and D can be set equal to zero without loss of generality, as this amounts to employing the variables $(y - C'z/E', z - D\alpha y/A)$ instead of (y, z) . Then, at $\tau'=0$, and for small values of α , i.e., for small x , the shell has a cusplike shape in the y - z plane, with sides given by

$$z = \pm E' \left| \frac{y}{A'} \right|^{3/2}. \quad (69)$$

B. Finite time rarefaction singularities

Let us now consider the hodograph transformed equations $\nabla\tau = \nabla\alpha \times \nabla\beta$ in the neighborhood of a rarefaction singularity (for the sake of simplicity, we assume that it is located at $\tau=0$, $\alpha=0$, and $\beta=0$, corresponding, with a proper redefinition of the coordinates, to $x=0$, $y=0$, and $z=0$). At this point the shell surface density goes to zero, and $\nabla\tau|_{(x=0,y=0,z=0)}=0$. Thus, at this singular point, we have

$$\nabla\alpha|_{(x=0,y=0,z=0)} \propto \nabla\beta|_{(x=0,y=0,z=0)}, \quad (70)$$

i.e., the surfaces $\alpha(x, y, z)$ and $\beta(x, y, z)$ are tangent at $(x=0, y=0, z=0)$.

Let us now specify an independent coordinate system such that, with the standard index notation, $x \equiv x_1$ lies along the common gradient direction; we expand α and β around the singularities

$$\alpha = ax_1 + A_{i,j}x_ix_j/2, \quad \beta = bx_1 + B_{i,j}x_ix_j/2. \quad (71)$$

With a suitable rotation in the α - β plane, and a rescaling, we can set $a=1$ and $b=0$. Keeping only linear terms in the product of the gradients, which corresponds to expanding τ up to quadratic terms, the compatibility condition $\nabla \times (\nabla\alpha \times \nabla\beta) = 0$ gives

$$B_{22} + B_{33} = B_{12} = B_{13} = 0. \quad (72)$$

Using these conditions and integrating $\nabla\tau$, we obtain

$$\tau = (B_{22} - B_{33})x_2x_3/2 - B_{23}(x_2x_2 - x_3x_3)/2, \quad (73)$$

i.e., τ is locally independent of x_1 and is harmonic in the perpendicular x_2, x_3 plane. With a rotation in the x_2 - x_3 plane, we can put the x_2x_3 term in the expression of τ equal to zero. Then we can reinterpret the above results in the forms

$$\beta = Cyz, \quad \tau = -C(y^2 - z^2), \quad (74)$$

$$\alpha = x + A_{i,j}x_ix_j/2, \quad (75)$$

where $C = B_{23}$, and β as a function of y and z , is the harmonic conjugate of τ .

We see also rarefaction singularities in three dimensions have a generic 2D character, and, as found in two dimensions, [see Eq. (56) of Ref. [2]], are described by two quadratic harmonic conjugate functions. Note that the case when both $\nabla\alpha$ and $\nabla\beta$ vanish at the singularity is nongeneric, and

is described by polynomial solutions of the types $\tau=xyz$, $\alpha=(x^2-y^2)/2$, and $\beta=(y^2-z^2)/2$ (see Sec. V). This latter solution has a 3D character, but is not structurally stable as its 3D structure is destroyed by making either $\nabla\alpha$ or $\nabla\beta$ arbitrarily small but not zero at the singularity.

VII. CONCLUSIONS AND DISCUSSIONS

In this paper we have investigated the problem of the formation of singularities in a thin shell in connection with the nonlinear development of the Rayleigh-Taylor instability of a plasma slab moving under the effect of a pressure term in the presence of a strong friction force. This work extends the two-dimensional analysis performed in Ref. [2].

In order to gain insight into the 3D nonlinear instability, we have used two main approximations. First, as in Ref. [2], we have restricted our analysis to the long wavelength limit where the plasma slab is modeled as a thin shell. Second, we have assumed that the pressure on the shell remains spatially homogeneous. We have shown that the different scaling with size from two to three dimensions causes the shell evolution equations to be structurally different from their 2D limit. In particular, they remain nonlinear when expressed in Lagrangian variables, contrary to the 2D case.

The resulting 3D equation has been shown to have interesting mathematical properties that make it possible to exhibit some of the nonlinear 3D behavior of the shell analytically, which is remarkable in view of the complexity of the problem. The formalism of the differential geometry is natural for this problem, and makes it possible to construct a generalization of the hodograph transformation.

We have shown that the 3D shell equations exhibit both compression and rarefaction singularities. A local analysis around the singular points has indicated that both finite time compression and rarefaction singularities in three dimensions have quasi-2D behaviors. The singularity develops along a curve on the shell and the dynamics of the shell, projected in the plane perpendicular to this curve at the singularity, is essentially the same as in two dimensions. Indeed, the coordinate along the curve plays the role of the ignorable coordinate of the 2D configuration. In particular, compression singularities develop a cusp structure that extends along the curve. Rarefaction singularities open along hyperbolae in the plane perpendicular to the curve. Genuine 3D singularities are possible, but have been shown to be structurally unstable.

The limitations of the validity of the long wavelength approximation were already discussed in Ref. [2], and remain essentially the same in three dimensions, that is, this approximation is better and better verified in the case of rarefaction singularities, while it must be interpreted as describing an intermediate asymptotics in the case of compression singularities.

The assumption of a spatially homogeneous pressure term is obviously more critical. If an inhomogeneity of the pressure term develops in time, additional nonlinearities are present and the shell evolution is altered, as indicated e.g., by Eq. (23). Nevertheless a regular, nonvanishing, inhomogeneous pressure term does not modify the 2D character of the singularities, which is a consequence of the vector nonlin-

earities of the shell equations. This can be seen by referring for example to the hodograph transformed equations. In the presence of an inhomogeneous pressure term, Eqs. (26) become

$$\mathcal{F}(\alpha, \beta, t) \nabla t = \nabla \alpha \times \nabla \beta, \quad (76)$$

where $\mathcal{F}(\alpha, \beta, t)$ is defined below Eq. (23). At the rarefaction singularities, where $\nabla t = 0$, the two vectors $\nabla \alpha$ and $\nabla \beta$ become tangent as in the uniform pressure case.

ACKNOWLEDGMENTS

This work was supported in part by the Italian Ministry for University and Scientific Research PRIN funds and by the Consiglio Nazionale delle Ricerche of Italy.

APPENDIX A: 1D GASDYNAMICS IN COORDINATE FREE FORM AND THE HODOGRAPH TRANSFORMATION

For a 1D fluid configuration, where quantities depend on x and t only, the continuity equation

$$\frac{\partial \rho}{\partial t} + \frac{\partial \rho u}{\partial x} = 0 \quad (A1)$$

and the Euler equation

$$\rho \left(\frac{\partial u}{\partial t} + u \frac{\partial u}{\partial x} \right) + \frac{\partial p}{\partial x} = 0, \quad (A2)$$

with density ρ , pressure $p = p(\rho)$, and enthalpy $h = h(\rho)$, can be written in the notation of differential forms as

$$d\rho \wedge dx = d(\rho u) \wedge dt, \quad (A3)$$

$$du \wedge dx = d(h + u^2/2) \wedge dt. \quad (A4)$$

Equations (A1) and (A2) follow by taking x and t as independent variables, and by expressing the dependent variables ρ and u as functions of x and t . Taking, instead, ρ and u as independent variables, and expressing x and t as functions of ρ and u , we obtain the hodograph transformed equations

$$\frac{\partial x}{\partial u} - u \frac{\partial t}{\partial u} + \rho \frac{\partial t}{\partial \rho} = 0, \quad (A5)$$

$$\frac{\partial x}{\partial \rho} + \frac{dh}{d\rho} \frac{\partial t}{\partial u} - u \frac{\partial t}{\partial \rho} = 0, \quad (A6)$$

which are linear in the dependent variables x and t .

APPENDIX B: SELF-SIMILAR SOLUTIONS WITH VELOCITY COMPONENTS LINEAR IN EULER COORDINATES

Self-similar solutions of the 3D equations (8) are obtained by setting

$$x^i = X_{a,b}^i(\tau) x_0^a x_0^b, \quad (B1)$$

where $x^i = x, y, z$ for $i = 1, 2, 3$ respectively, x_0^a are the Lagrangian variables α and β for $a, b = 1, 2$, respectively, and $X_{a,b}^i(\tau)$ are three linearly independent 2×2 symmetric real matrices that are functions of time and whose coefficients satisfy the system of nine coupled ordinary differential equations

$$\dot{X}_{a,b}^i = 2 \epsilon^{ijk} (X_{a,1}^j X_{2,b}^k + X_{b,1}^j X_{2,a}^k), \quad (\text{B2})$$

where the dot denotes a derivative with respect to τ , and ϵ^{ijk} is a completely antisymmetric Ricci tensor. Expressing the symmetric matrix product on its right-hand side as a time dependent combination of the three linearly independent symmetric matrices $X_{a,b}^i$, we see that Eq. (B1) corresponds to solutions where the velocity components are linear, time dependent functions of the Eulerian coordinates x, y , and z . In these solutions the variables α and β are simply labels, and cannot be interpreted as initial coordinates, and the shell surface density tends to infinity for $x = y = z = 0$ as $1/R$.

Taking $a = b = 1$ in Eq. (B2) and then $a = b = 2$, we obtain

$$\dot{X}_{1,1}^i = 4 \epsilon^{ijk} X_{1,1}^j X_{2,1}^k \quad \text{and} \quad \dot{X}_{2,2}^i = 4 \epsilon^{ijk} X_{2,1}^j X_{2,2}^k, \quad (\text{B3})$$

which give

$$\sum_i (X_{1,1}^i)^2 = \text{const} \quad \text{and} \quad \sum_i (X_{2,2}^i)^2 = \text{const}. \quad (\text{B4})$$

Instead taking $a = 1$ and $b = 2$, we obtain

$$\dot{X}_{1,2}^i = 2 \epsilon^{ijk} X_{1,1}^j X_{2,2}^k, \quad (\text{B5})$$

which, together with Eqs. (B3), give

$$\sum_i X_{1,1}^i X_{1,2}^i = \text{const},$$

$$\sum_i X_{2,2}^i X_{1,2}^i = \text{const},$$

(B6)

$$\sum_i [X_{1,1}^i X_{2,2}^i + 2(X_{1,2}^i)^2] = \text{const},$$

$$\sum_i (\dot{X}_{1,1}^i X_{2,2}^i - X_{1,1}^i \dot{X}_{2,2}^i) = 0.$$

In Eulerian coordinates the above equations correspond to the orthogonality condition

$$\mathbf{v} \cdot \mathbf{r} = 0,$$

i.e., to

(B7)

$$x^2 + y^2 + z^2 = \text{const}.$$

Thus the shell motion corresponds to a complex rotational motion around a time dependent axis. An elementary solution is given by the case when all functions X are zero except $X_{1,1}^1 = \sin \tau$, $X_{1,1}^2 = \cos \tau$, and $X_{1,2}^3 = 1/4$.

More general self-similar solutions can be obtained by adding, to Eq. (B7) a time dependent linear term in the Lagrange coordinates α and β and a time dependent constant term, as done, e.g., in Ref. [11]. The equations that determine the time behavior of these additional terms depend on the functions X , while Eqs. (B2) remain unchanged.

-
- [1] E. Ott, Phys. Rev. Lett. **29**, 1429 (1972).
 [2] S.V. Bulanov, F. Pegoraro, and J.-I. Sakai, Phys. Rev. E **59**, 2292 (1999).
 [3] W. Manheimer, D. Colombait, and E. Ott, Phys. Fluids **27**, 2164 (1984).
 [4] T. Taguchi and K. Mima, Phys. Plasmas **2**, 2790 (1995).
 [5] M.M. Basko, Phys. Plasmas **1**, 1270 (1994).
 [6] R. Bingham, R. Bollens, F. Kazeminejad, and J.M. Dawson, Cometary Plasma Proc. **61**, 73 (1991).
 [7] S.V. Bulanov and P.V. Sasorov, Fiz. Plazmy **4**, 746 (1978) [Sov. J. Plasma Phys. **4**, 418 (1978)].
 [8] N.A. Krall and A.W. Trivelpiece, *Principles of Plasma Physics* (McGraw-Hill, New York, 1973).
 [9] H. Flanders, *Differential Forms with Applications to the Physical Sciences* (Dover, New York, 1989).
 [10] R. Courant and K.O. Friedrichs, *Supersonic Flow and Shock Waves* (Interscience, New York, 1948).
 [11] S.V. Bulanov and M.A. Ol'shanetskij, Fiz. Plazmy **11**, 727 (1985) [Sov. J. Plasma Phys. **11**, 425 (1985)].
 [12] S.V. Bulanov, F. Pegoraro, and A.S. Sakharov, Phys. Fluids B **4**, 2499 (1992).
 [13] L.D. Landau and E.M. Lifshitz, *Quantum Mechanics* (Pergamon Press, New York, 1965), Sec. 37.
 [14] D. Lynden-Bell, Mon. Not. R. Astron. Soc. **124**, 9 (1962).
 [15] V.I. Arnol'd, *The Catastrophe Theory* (Nauka, Moscow, 1990).